IOP Conference Series: Earth and Environmental Science

PAPER • OPEN ACCESS

Enhancing the Urban Atlas Features with the Water Balance Estimates Using the Landsat 8 Imagery

To cite this article: Douraied Guizani *et al* 2023 *IOP Conf. Ser.: Earth Environ. Sci.* **1189** 012027

Enhancing the Urban Atlas Features with the Water Balance Estimates Using the Landsat 8 Imagery

Douraied Guizani[1], Erika Buday-Bódi[1*], János Tamás[1] and Attila Nagy[1]
[1] Institute of Water and Environmental Management, Faculty of Agricultural and Food Sciences and Environmental Management, University of Debrecen, H-4032 Debrecen, Böszörményi str. 138.

Correspondence: bodi.erika@agr.unideb.hu (E.B.B.)

Abstract. Between climate change and anthropogenic forcing, pressure on water resources is continually increasing all over the world. The growing population is gathering more and more in cities where the artificialization of soils and urban developments of all kinds are modifying the local water cycle. However, knowledge about the hydrological cycle in urban areas is not well developed today. Urbanization in a watershed can produce significant changes to the natural water cycle, mainly because permeable soils have been covered by less permeable surfaces. The consequences of this urbanization can be significant and multiple. The assessment of urban water resources aims to provide a suitable circumstances for planning, conditions for the planning, design, construction, operation, and maintenance of works used for irrigation and sanitation, among other applications. The methodology of the research is based on the data collection, which includes climatic data from June 2021 to June 2022 and the use of Digital elevation model to create a hydrographic network. The second part is land use data processing to create a land cover map using maximum Likelihood Supervised Classification, by combining different band composites of Landsat 8 images and NDVI to differentiate between vegetative and non-vegetative areas. However, CORINE Land Cover database was utilized to distinguish between continuous and discontinuous urban area in this classification. The final step in the process is to determine the hydrological coefficients by calculating the water cycle parameters (Evapotranspiration Runoff and Infiltration) for each land-use class. Furthermore, establishing a link between land use and hydrological behaviour and conducting a precise calculation of water balance-related coefficients in urban areas using Urban Atlas 2018.

1. Introduction

Water is a natural resource essential to the survival of populations and to the prosperity of their agricultural, industrial, and therefore economic activities. Despite that earth is the Blue Planet, it is water that is most lacking to Humanity (Goude, 2011).

The growing population is converging on cities, where soil artificialization and various types of urban development are altering the local water cycle (Vrebos et al., 2014).

In a watershed, urbanization can significantly change the natural water cycle (Seto et al., 2011). However, today's urban knowledge of the hydrological cycle is limited and there is still a lack of compatible data suitable for the generation of topical information about the urbanised water parameters and its changes at different scales (Askarizadeh et al., 2015). Furthermore, precise, and small-scale urban water balance computations are not widely developed (Wortman and Lovell, 2013).

In this context, the necessity for this research is that efficient urban water management requires a comprehensive understanding of anthropogenic impacts on the urban hydrological cycle and the environment. Such effects vary widely in time and space, and must be assessed in relation to local climate, urban growth, cultural and environmental, as well as other socioeconomic aspects.

The European Environmental Agency developed the GIS database Urban Atlas, which includes geographical and statistical information for 800 functional urban areas across Europe, including information on the population, area, and LULC types for various land cover patches. Urban Atlas is extensively used by scholars since it is freely accessible and has great resolution. (Barranco et al., 2014; Akay and Sertel, 2016; Pazúr et al., 2017; Poleman, 2018; Kukulska-Kozieł et al., 2019).

The aim of this work was to investigate the relationships between Land Use Land Cover and the water cycle parameters by developing a spatial decision support system for water balance modelling that merged geographic information systems (GIS) and remote sensing (RS). Using climatic data from June 2021 to June 2022, the ET (Evapotranspiration) was calculated. The estimated Evapotranspiration, runoff and Infiltration were added as an attribute to LULC of urban Atlas. The study place is Debrecen, in northeastern Hungary. The approach taken in this study can be applied in other cities.

2. Materials and methods

To perform more accurate water balance calculations, the study was to identify and link the most crucial parameters to the LULC categories, such as crop coefficients for estimating crop ET (ETc) and runoff coefficients for calculating infiltration rate.

Our forward-looking research approach consists primarily of decide the orientation of the mapping: study area, geographic projection, mapping of Land cover and identify needs and data sources, then data collection and documentation by creating a database and developing metadata and the preparation of input data: development of GIS databases, GIS operations, digital terrain analysis, and image analysis covering the study area.

The second stage is constituted for the establishment of relations between land cover and different hydrological parameters. In the third step, a model developed to estimate the average annual water balance of different surfaces, the model describes the mean annual values of surface runoff, Infiltration, and evapotranspiration as portions of the rainfall.

2.1 Description of the study site

With a total area of 461.25 km2 and a population of 200 000, Debrecen is Hungary's second-largest city after Budapest, located on the Great Hungarian Plain, 220 kilometers east of the capital Budapest. The Aster database indicates that Debrecen's elevation ranges from 97 to 161 meter (Figure 1).

The precipitation in the area of interest throughout the year due to its humid continental climate. The average yearly precipitation between June 2021 and June 2022 was 465 mm. In this area, the precipitation is the factor that varies the most. For instance, the National Weather Service's meteorological data indicates that between June 2021 and June 2022 the wettest month was July (75 mm), whereas the driest month were June (15.89 mm).

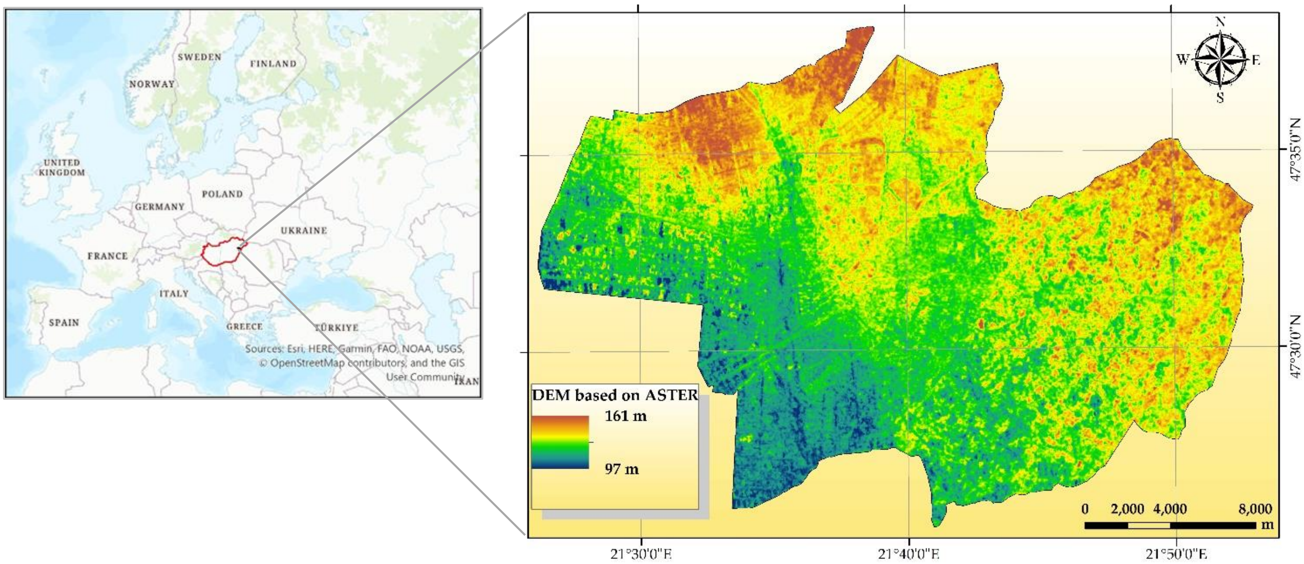

Figure 1. Location of the study region and the Digital Elevation Model (DEM) (sources: Open Street Map (Esri, HERE, Garmin, FAO, NOAA, and USGS).

2.2 Data

In this study Landsat 8 image service was used for NDVI (Normalized Difference Vegetation Index) calculation. ASTER data have been enhanced to provide digital elevation data used to determining the hydrographic network. The layer for administration area of Debrecen was acquired from the National Regional Development and Spatial Planning Information System ("TEIR"). Urban Atlas vector 2018 was downloaded from the site of the European Union's Earth observation programme Copernicus. The climatic data was obtained from the Hungarian National Climatic Service (in Hungarian: OMSZ), for the period between the years 2016 and 2019.

2.3 Methods

2.3.1 Urban vegetation mapping based on NDVI

These land classes are based on the NDVI values, classified into non-vegetation (-1 to 0.199), low vegetation (0.2 to 0.5) and high vegetation (0.501 to 1.0) (Haslina et al., 2019).

The normalized difference vegetation index (NDVI) is a considerable technique employed to signal out any possible changes in the land. The calculation of Normalized difference vegetation index NDVI of Debrecen shows that the areas without vegetation (non-vegetation class) such as water surfaces, as well as urban areas and bare lands are represented with very low NDVI values, while the dense vegetation area presents high NDVI values (Tucker, 1979). The comparison between summer and winter NDVI is presented in Figure 2.

For Land use classification, the processed data was divided into 3 major levels:

- Image pre-processing
- NDVI threshold
- Classification of urban vegetation types.

The first step is to correcting and processing the imagery. Afterwards, the selection of NDVI value for vegetation mapping is conducted. According to the NDVI, specified classes categorize the imagery based on supervised classification. NDVI execution values are ranging from -1 to 1 and used to reclassify the maps to refer to vegetation rates, resting on spectral reflections (Kumar et al., 2015).

2.3.2 Hydrological coefficient

Evapotranspiration coefficient

The average annual temperature and precipitation over the period of time between July 2021 and July 2022 are used to determine the evapotranspiration coefficient by land use and land cover category in the watershed. Second, the Turc formula (Turc, 1961) is used to assess the average annual evapotranspiration. Then we use the crop coefficients, provided by the FAO bulletin (Food and Agriculture Organization), to calculate the actual evapotranspiration for the land cover classes of the watershed.

$$E = \frac{P}{\sqrt{0.9 + \frac{P^2}{L^2}}} \quad (1)$$

Whereas:

- $L = 200 + 25t + 0.05t^3$
- E or ET0: the reference evapotranspiration (mm/ year).
- P: the annual precipitation (mm).
- t: mean annual temperature (°C).
- The minimum mean annual temperature (Tmin) is 6.4 ° C.
- The maximum mean annual temperature (Tmax) is 17.3 ° C.
- The annual precipitation P is 465.45 mm.

By combining Turc formula, P, tmin and tmax we obtained the minimum and maximum values of the average annual reference evapotranspiration of the Basin:

$$ET_{\circ}\,min = \frac{P}{\sqrt{0.9 + \frac{P^2}{Lmin^2}}} \quad (2)$$

- $Lmin = 200 + 25\ tmin + 0.05tmin^3 = 298.36\ mm\ (64\%\ of\ total\ precipitation\ )$

Maximum mean value:

$$ET_{\circ}\,max = \frac{P}{\sqrt{0.9 + \frac{P^2}{Lmax^2}}} \quad (3)$$

- $Lmax = 200 + 25\ tmax + 0.05tmax^3 = 429\ mm\ (92\ \%\ of\ total\ precipitation\ )$

Evapotranspiration evaluation for Land use and Land cover categories

The crop evapotranspiration (ETc.) is calculated by the following formula (Wang et al., 2018):

$$\text{ETc} = \text{Kc x ET0} \quad (4)$$

- ETc: maximum crop evapotranspiration (in mm).
- Kc: crop coefficient (dimensionless).
- ET0: reference evapotranspiration (in mm).

The FAO bulletin (Allen et al., 1998) provides the crop coefficients kc in tabular form for the various species based on the stage of development. Tallis et al. (2013) generated crop coefficient values. These values were employed in the investigation. The evapotranspiration coefficients can be used to non-vegetated classes such bare soil or water bodies, based on FAO report. In general, waterproof surfaces are given a very low coefficient Kc value, focusing attention instead on the drainage procedure.

On the other hand, water that is stationary or moves slowly is given a coefficient that is near to 1 (Richard et al., 1998).

We will evaluate the evapotranspiration coefficients (ET_{cn}) for each of LULC classes in this study. Finding a crop coefficient for each land use type (K_{cn}) is necessary to do this.

For each land use class in the Debrecen basin, the evapotranspiration calculation is shown in the following equation.

$$ET_{cn} = K_{cn} * ET_0 \quad (5)$$

- n: land use category ID (n = 1…8)
- K_{cn}: crop coefficient by land use category
- ET_0: average annual reference evapotranspiration (mm)

Determination of the crop coefficients of LULC categories

The crop coefficients (k_c) from Tallis et al. (2013) and Allen et al. (1998) cannot be used directly because they were developed for homogeneous vegetation types. Therefore, in our study case, we went through the following process to estimate the crop coefficients (K_c) of the Debrecen city classes: First, homogenous classes were determined and provided in Allen (1998) and Tallis (2013), after which the average of those values was calculated to recreate the Debrecen city classes (Bare ground, Forest, water bodies, Grassland, Crop cover area, Discontinuous and continues Urban). Irrigation and horticulture handbooks contain values for the evapotranspiration coefficient (K_c) for crops. An online resource for this from FAO is at https://www.fao.org/3/X0490E/x0490e0b.htm.

Table 1. Cropping coefficients (K_c) for Debrecen LULC. (Tallis et al. (2013); Allen et al. (1998)).

Land Use Land Cover	k_c
Forest	1
water bodies	1.2
Continuous Urban	0.001
Bare Ground	0.001
Area with crop cover	0.783
Discontinuous urban	0.26
Grassland	0.833

Estimating the proportion of evapotranspiration for various land use and land cover types

We apply the following equation to get the Water deficit for the watershed LULC categories:

$$ET_{cn\,max} = \frac{K_{cn} * ET_{\circ}max}{P} * 100 \quad (6)$$

$$ET_{cn\,min} = \frac{K_{cn} * ET_{\circ}min}{P} * 100 \quad (7)$$

- $ET_{\circ max}$: the Maximum mean reference evapotranspiration (%)
- $ET_{\circ min}$: the Minimum mean reference evapotranspiration (%)

- $ET_{cn\ min}$: the Minimum average reference evapotranspiration of the LULC categories (%).
- ET_{cn} max: the Maximum mean reference evapotranspiration of the LULC categories (%).
- K_{cn}: the Crop coefficient for the LULC categories.
- P: the annual precipitation (in mm).

2.3.3 Runoff coefficient

To estimate the runoff coefficients for the Debrecen city classes, we use various publications (Table 2) presenting estimates of the values of the runoff coefficient by type of land use. Some authors gave the result of the runoff coefficient as an interval (minimum value and maximum value) and others gave the result of the runoff coefficient as a single digit for different types of land use.

In order to determine the runoff coefficient for the classes in our study watershed, we first searched for references that had LULC categories comparable to those in our study area (Table 2). In the second step, we determined the average value of all the runoff values stated in the references.

Water infiltration amounts vary depending on a number of variables, including the soil's composition and surface features. For this purpose we apply the balancing equation with a new unknown, infiltration by land use class, to compute the infiltration volume by land use classes.

Table 2. Bibliographic sources used to calculate runoff values

Land use class	Average Annual Runoff (%)	Bibliographical references
Continuous urban site	74.42	The COMET® Program, 2010 / LINDERBERG, 1999 /SARUKKALIGE MALCOM, 1997 ... Town of Buckeye Public Works Department, 2007/DRUAIS, 2009/..
Discontinuous urban	66. 04	LINDEBERG, 1999 / FERGUSON-THOMAS, 1990/ BROWN-STEIN-WARNER, 1996 …
Agricultural area - vegetated	25.67	The COMET® Program, 2010/ SARUKKALIGE, 2011/ FERGUSON-THOMAS…
Grassland	25	The COMET® Program, 2010/ LINDEBERG, 1999/ VIESSMAN-LEWIS, 1996…
secondary vegetation	17.19	LINDERBERG, 1999/ SARUKKALIGE, 2011 The COMET® Program, 2010 …
Forest	9.1	The COMET® Program, 2010/ LINDERBERG, 1999/ VIESSMAN-LEWIS, 1996…
Agricultural area Bare soil	63.75	FERGUSON-THOMAS, 1990/ Town of Buckeye Public Works Department, 2007…
Water and wetland		--

3. Results

3.1. NDVI calculations and analysis

Debrecen in summer presents an NDVI of the order of 0.8 (Figures 2a) and 2b) which explains the strong vegetation presented by the dominance of green colour at the level of the map.

Debrecen in the winter months shows an NDVI of around 0.15 with a less intense distribution of green color which explains the existence of low vegetation. The NDVI values vary according to the four seasons of the year. Specifically, these values are different in the summer and winter seasons. As indicated in the Figure 2c) and Figure2d), the greenness density reaches high and remarkable levels in the summer, compared to lower levels in the winter. The variation in the greenness level is indicative of the state of vegetation during specific periods of the year. All in all, these figures represent the NDVI of 2019 only. So, the obtained greenness levels are true only for this specific period of the year. Any potential reversal in the greenness levels may be due to severe climatic changes and anthropogenic activities.

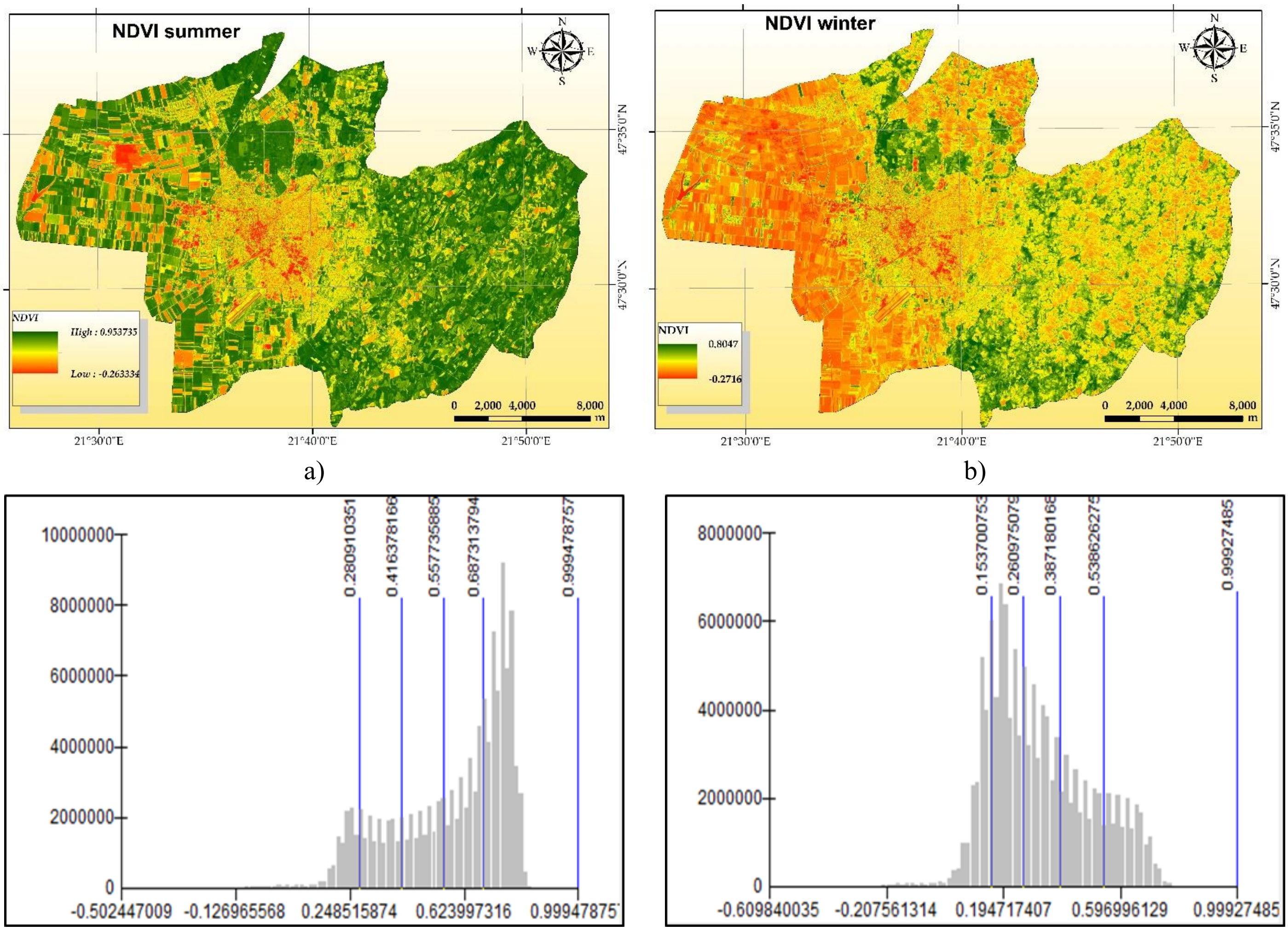

a) b)

c) d)

Figure 2. Normalized Difference Vegetation Index (NDVI) maps of Debrecen for summer (a) and winter (b) and the related histograms (c) and (d), respectively.

3.2. *Landsat based LULC map of Debrecen*

As shown in the following Figure 3, land use varies considerably from one area to another. In fact, forests cover the entire northern and eastern part, while pastures have the highest percentage of land cover in the watershed. The urban area is mainly concentrated in the center of the basin. The supervised classification tool in ArcGIS, which displays land classes like land-use type, was used to create this map of the land cover. Pixels in polygons serve as a unique identifier for this raster. The accuracy of the final obtained land cover increases with the number of land use samples provided for the classification.

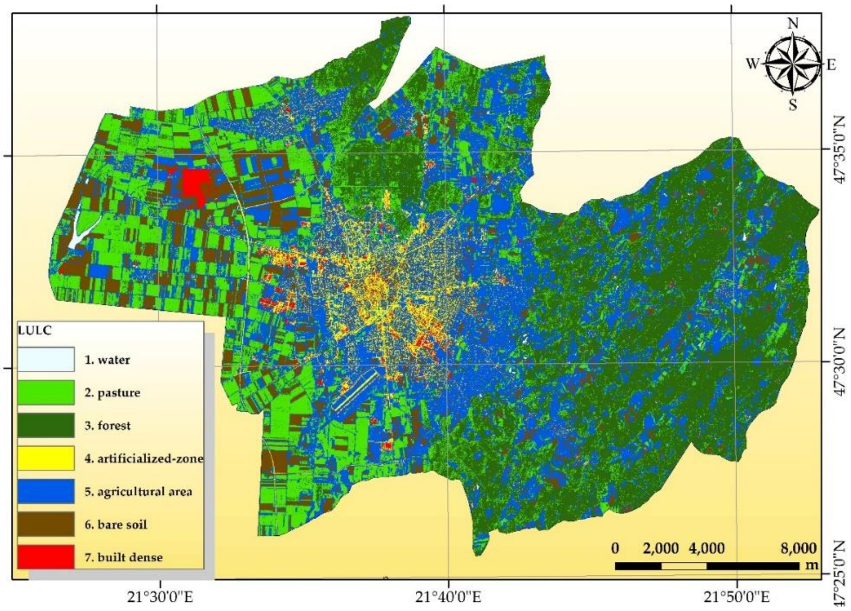

Figure 3. Landuse classification of Debrecen

The Kappa coefficient provides details on the classification of pixels made by random and shows the accuracy of the classification. According to Landis and Koch (1977), it ranges from -1 to 1, and the higher the Kappa coefficient, the higher the quality (Congalton, 1991).

Overall Accuracy = $\frac{total\ Number\ of\ correctly\ classified\ pixels\ [\ Diagonal]}{total\ Number\ of\ Reference\ pixels} * 100$; (Ma and Redmond 1995) (8)

Users Accuracy = $\frac{Number\ of\ correctly\ classified\ pixels\ in\ eatch\ category}{total\ numbers\ of\ classified\ pixels\ in\ that\ category\ [\ row\ total]} * 100$ (Rosenfield and Fitzpatrick-Lins, 1986) (9)

Producers Accuracy = $\frac{Number\ of\ correctly\ classified\ pixels\ in\ eatch\ category}{total\ numbers\ of\ classified\ pixels\ in\ that\ category\ [\ column\ total]}$*100 (Nasset 1995) (10)

$$K=\frac{N\sum_{i=1}^{r}X_{ii}-\sum_{i=1}^{r}X_{i+}.X_{+i}}{N^2-\sum_{i=1}^{r}X_{i+}.X_{+i}} \quad (11)$$

- K: Kappa coefficient.
- N: The total number of samples.
- ii: Is the number of observations in row I and column.
- i, X_(+i) : the marginal totals of column.
- i, X_(i+) : the marginal totals of row I.

Overall classification accuracy was good (81.2%), and all Kappa coefficients were over 0.78. These statistics presume that our classifications are significant and reasonably near to the reality shown in

Google Earth photos according to our supervised categorization, based on the Kappa scale provided by Landis and Koch (1977).

3.3. Hydrological parameters

It is crucial to note that the research area's topography is generally flat and because of the high biomass and vitality in summer period (July), the LULC map is obtained; however, the plant cover can change during other seasons of the year (Hüse et al., 2016).

Table 3. Hydrological parameters by LULC category

LULC	**Evapotranspiration ratio**		**Infiltration ratio P- (ET ratio + Runoff)**
	(Min-max) %	**(Average)%**	**(Average) %**
Forest	64.1-92.1	78.1	12.8
Area with crop cover	50.1-72.1	61.17	13.16
Grassland and pasture	53.4-76.7	65	15
Discontinuous urban	16.6-23.9	18.6	15.36
Continuous Urban	0.065-0.023	0.044	25.5
Bare ground	0.065-0.023	0.044	25.5
Surface water bodies	76.9-100	88.45	-

The significance of this study is that, despite changes in crop patterns, the computation and validation process can be applied to other locations and other time periods. The results of the Hydrological parameters per LULC category for the Debrecen basin is presented in Table 3. The infiltration ratio is obtained based on the following equation I% =100- (ET%+Runoff Coefficient %).

3.4. Precise Evapotranspiration, Runoff, and Infiltration attributes of Urban Atlas LULC categories

The following Figure 4 provides an overview of the central and urban core of Debrecen basin, along with the surface of every land cover type. Based on the prepared LULC map we calculated the hydrological parameters of an official land cover map from Urban Atlas (https://land.copernicus.eu/local/urban-atlas). This descriptive information is obtained via zonal statistic function summarizes the values of a raster within the zones of another dataset and report the results as a table.

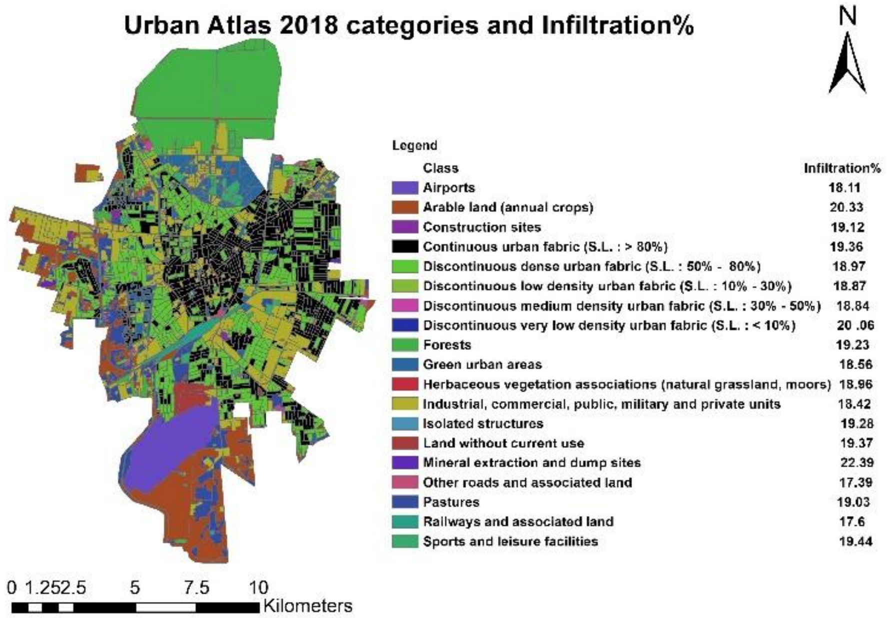

Figure 4. Urban Atlas LULC categories of the central and urban core of Debrecen basin (S. L. refers to Sealing Layer)

Table 4. Hydrological parameters for the urban core of Debrecen

Class_2018	Area	ET	Runoff	Infiltration	
	%	%	%	%	STD
Airports	29.25	45.62	35.26869061	18.11826929	2.680499969
Arable land (annual crops)	2.73	49.02	29.64716764	20.3300255	3.731067791
Construction sites	0.37	26.52	53.34914361	19.1284585	4.368406049
Continuous urban fabric (S.L. : > 80%)	0.078	31.51	48.16566834	19.36779308	5.071226335
Discontinuous dense urban fabric (S.L. : 50% - 80%)	0.077	38.20	41.82230653	18.97799766	4.371906815
Discontinuous low density urban fabric (S.L. : 10% - 30%)	0.011	44.90	35.2184769	18.87640449	3.481135903
Discontinuous medium density urban fabric (S.L. : 30% - 50%)	0.09	44.90	35.24925373	18.84378109	3.567051214
Discontinuous very low-density urban fabric (S.L. : < 10%)	0.019	35.10	43.83624454	20.06113537	5.036176595
Forests	28.66	67.28	12.48220904	19.23559981	0.728754204
Green urban areas	0.05	55.26	25.21217724	18.56951473	1.895375792
Herbaceous vegetation associations (natural grassland, moors...)	0.01	60.16	19.87272727	18.96363636	1.306816206
Industrial, commercial, public, military and private units	0.011	26.04	54.57716805	18.42671316	4.277423642
Isolated structures	0.04	47.27508455	32.43517475	19.2897407	3.328761046
Land without current use	0.03	48.37399435	31.2469015	19.37910415	3.716454129
Mineral extraction and dump sites	0.21	23.02559415	53.57678245	22.3976234	4.979669253
Other roads and associated land	36.36	34.44247702	47.1701016	17.39622642	3.408922139
Pastures	0.12	50.51926837	29.44989746	19.03083417	2.936211276
Railways and associated land	0.013	38.40534856	43.00120192	17.60386619	3.126606811
Sports and leisure facilities	1.817	38.93638677	41.06177552	19.44656489	4.0891656

Data presented in Table 4 indicates that mineral extraction and dump sites, arable land (annual crops) and discontinuous very low-density urban fabric (S.L.: < 10%) have the highest infiltration percentage being 22.39%, 20.33%, and 20.06%, respectively. These infiltration amounts are paralleled with runoff percentage that equal 53.57%, 29.64%, and 43.83%, and evapotranspiration rate that equal 23.02%, 49.02%, and 35.1%. In these land class types, there is no or limited waterproof surface. Such a fact augments the infiltration amounts. Moreover, the high runoff amounts are explained by the lack of vegetation that helps in reducing water runoff. A good example of a limited runoff rate is detected in forests (12.48%), green urban areas (25.21%) and herbaceous vegetation associations (natural grassland, moors...) (19.87%), which accentuates the role of vegetation in limiting water runoff. The infiltration values in other roads and associated land (17.39%), railways and associated land (17.6%), airports (18.11%), and industrial, commercial, public, military, and private units (18.42%) are very low in comparison with other green areas. These limited values are due to the existence of extended waterproof areas. Such a fact contributes to increasing the runoff values, being 47.17%, 43%, and 54.57%, which respectively comply with the aforementioned areas.

4. Conclusion

The integrated management of water resources is a complicated field that necessities for collecting much of data and developing a cohesive understanding of how natural systems interact with specific socio-hydro systems components. Particularly significant are the connections between major hydrological processes of the water cycle and land use categories.

Applying the "Maximum Likelihood" supervised classification method, images having a Kappa coefficient greater than 81% may be categorized. In this study, we investigated the possibility of using the Google Earth tool to keep an eye on LULC classes. The relationships between the main hydrological processes of the water cycle and land use are particularly crucial. Here, are working on a technique for building a GIS that will be used to analyze the spatio-temporal development of land use and its effects on the key hydrological processes of the water cycle at the size of hydrographic basins. Using annual maps of evapotranspiration, runoff, and infiltration, these effects are evaluated.

This study presents novel perspectives on how to apply this methodology for watershed-scale integrated management of water resources and land use planning. It is intended to be adjusted to the problems and limitations (particularly observational) associated with the management of hydrographic basins and where the availability of water can have a scarce quality that is emphasized by competing uses. The method's adaptability, quick implementation, and lack of need for massive modeling equipment or a diverse set of abilities are all advantages for its application. This work also has the potential to test several future hypotheses regarding climatic change and changes in land cover.

Acknowledgments: This study was supported by the National Research, Development and Innovation Office of Hungary (under grant: National Laboratory of Water Science and Water Safety project RRF-2.3.1-21-2022-00008).

5. References

1. Allen R.G, Pereira L.S, Raes D, and Smith M. (1998): Crop Evapotranspiration-Guidelines for computing crop water requirements-FAO Irrigation and drainage paper 56. FAO Rome, 300, D05109.

2. Akay and Sertel, 2016 S.S. Akay, E. Sertel Urban Land cover/use Change Detection Using High Resolution Spot 5 and Spot 6 Images and Urban Atlas Nomenclature XLI-B8 (2016), pp. 1-8, https://doi.org/10.5194/isprsarchives-XLI-B8-789-2016

3. A. Askarizadeh, M.A. Rippy, T.D. Fletcher, D.L. Feldman, J. Peng, P. Bowler, A.S. Mehring, B .K. Winfrey, J.A. Vrugt, A. Aghakouchak, S.C. Jiang, B.F. Sanders, L.A. Levin, S. Taylor, S.B. Grant. From rain tanks to catchments: use of low-impact development to address hydrologic symptoms of the urban stream syndrome. Environ. Sci. Technol., 49 (2015), pp. 11264-11280, https://doi.org/10.1021/acs.est.5b01635

4. Brown S.A, Stein S.M, Warner J.C. (1996): Urban Drainage Design Manual. Hydraulic Engineering Circular 22, FHWA-SA-96-078, *Federal Highway Administration, U.S. Department of Transportation Washington*, DC, 478p. https://www.fhwa.dot.gov/engineering/hydraulics/pubs/10009/10009.pdf

5. Bourrier R. (1997): Les Réseaux D'assainissement: Calculs, Applications, Perspectives. Lavoisier, Technique et Documentation. Paris, ISBN: 978-2-7430-1051-5 (5th edition), 1002p.

6. Barranco et al., 2014 R.R. Barranco, F.B.E. Silva, M. Marin Herrera, C. Lavalle, Integrating the MOLAND and the urban atlas geo-databases to analyze urban growth in european cities. J. Map Geogr. Libr., 10 (2014), pp. 305-328, https://doi.org/10.1080/15420353.2014.952485

7. Bharathkumar, L, & Mohammed-Aslam, M. A. (2015) Crop pattern mapping of tumkur taluk using NDVI technique: a remote sensing and GIS approach. Aquatic Procedia, 4, 1397- 1404.

8. Congalton, R.G. (1991): A Review of Assessing the Accuracy of Classifications of Remotely Sensed Data. *Remote Sensing of Environment*, 37, 35-46. https://doi.org/10.1016/0034-4257(91)90048-B

9. DEPARTEMENT DU TERRITOIRE (République et canton de Genève) (2005): Gestion quantitative des eaux pluviales: Méthode simplifiée pour le dimensionnement et la conception des ouvrages de rétention pour les petits bassins versants urbanisés. Version 1.1, p 25: https://www.ge.ch/document/13223/telecharger

10. Goudet J. L, (2011): L'eau, première cause de mortalité dans le monde. *Futura-Sciences*.

11. Poleman H. (2018) A Walk to the Park? Assessing Access to Green Areas in Europe's Cities. Update Using Completed Copernicus Urban Atlas Data

12. Haslina H, Zulkiflee A , Nor A (2019): Urban vegetation classification with NDVI threshold value method value method with very high resolution (VHR) Pleiades imagery : *The International Archives of the Photogrammetry, Remote Sensing and Spatial Information Sciences*,

Volume XLII-4/W16, 2019 6th International Conference on Geomatics and Geospatial Technology (GGT 2019), 1–3 October 2019, Kuala Lumpur, Malaysia

13. J. Richard Landis and Gary G. Koch (1977): The Measurement of Observer Agreement for Categorical Data. Vol. 33, No. 1, pp. 159-174. *International Biometric Society*. https://www.jstor.org/stable/pdf/2529310.pdf

14. Kukulska-Kozieł et al., 2019. A. Kukulska-Kozieł, M. Szylar, K. Cegielska, T. Noszczyk, J. Hernik, K. Gawroński, R. Dixon-Gough, S. Jombach, I. Valánszki, K. Filepné Kovács. Towards three decades of spatial development transformation in two contrasting post-Soviet cities—kraków and Budapest. Land Use Policy, 85 (2019), pp. 328-339, https://doi.org/10.1016/j.landusepol.2019.03.033

15. Rosenfield, G.H. and Fitzpatrick-Lins, K., 1986. A coefficient of agreement as a measure of thematic classification accuracy. Photogram. Eng. Remote Sensing, 52: 223-227.

16. Shinde PG. (2005.): Water scenario 2025. National Level Conference on Water Management Scenario 2025 Problems, Issues and Challenges, January 21, 2005. India.
17. Seto, K. C., Fragkias, M., Güneralp, B., & Reilly, M. K. (2011). A meta-analysis of global urban land expansion. PLoS ONE,6(8), e23777.PubMedCrossRefGoogle Scholar https://link.springer.com/chapter/10.1007/978-94-007-7088-1_1#:~:text=Seto%2C%20K.%20C.%2C%20Fragkias,Google%20Scholar

18. Wortman S.E., Lovell S.T. (2013) Environmental challenges threatening the growth of urban agriculture in the United States, J Environ Qual. 2013 Sep;42(5):1283-94. https://doi.org/10.2134/jeq2013.01.0031

19. Tallis H. T. - Ricketts T. - Guerry A. D. - Wood S. A. - Sharp R. - Nelson E. - Ennaanay D. - Wolny S. - Olwero N. - Vigerstol K. - Pennington D. - Mendoza G. - Aukema J. - Foster J. - Forrest J. - Cameron D. – Arkema K. - Lonsdorf E. - Kennedy C. - Verutes G. - Kim C. K. - Guannel G. - Papenfus M. - Toft J. - Marsik M. - Bernhardt J. - Griffin R. – Glowinski K. - Chaumont N. - Perelman A. - Lacayo M. - Mandle L. - Griffin R. - Hamel P. - Chaplin-Kramer R. (2013): A modeling suite developed by The Natural Capital Project to support environmental decision- making, *InVEST 3.0.0 User's Guide: Integrated Valuation of Environmental Service and Tradeoffs*. The Natural Capital Project, Stanford, CA.

20. Turc L., (1961): Estimation of irrigation water requirements, potential evapotranspiration: a simple climatic formula evolved up to date. Annals of Agronomy 12: 13-49.

21. THE COMET ® PROGRAM (2010): Runoff Processes: International Edition. University Corporation for Atmospheric Research.

22. TOWN OF BUCKEYE PUBLIC WORKS DEPARTMENT (2007): Drainage Design Manual: Storm Water Drainage System Design Town of Buckeye. August 2011, 70p. https://www.buckeyeaz.gov/home/showpublisheddocument/442/636430710421630000

23. Thibaut C. (2004). Coefficients de ruissellements extraits de Etude hydrologique du bassin du Roua. http://www.aude.gouv.fr/IMG/pdf/rn18-026-impact_hydro_payra_v4.pdf

24. Vrebos D. - Vansteenkiste T. - Staes J. - Willems P. - Meire P. (2014): Water displacement by sewer infrastructure in the Grote Nete catchment, Belgium, and its hydrological regime effects. Hydrology and Earth System Sciences 18(3): 1119-1136.

25. Vrebos D. - Vansteenkiste T. - Staes J. - Willems P. - Meire P. (2014): Water displacement by sewer infrastructure in the Grote Nete catchment, Belgium, and its hydrological regime effects. Hydrology and Earth System Sciences 18(3): 1119-1136.

26. Ma, Z. and Redmond, R.L., (1995): Tau coefficient for accuracy assessment of classification of remote sensing data. Photogram. Eng. Remote Sensing, 61: 435-439.

27. Naesset, E., 1995. A method to test for systematic differences between maps and reality using error matrices. Int. J. Remote Sensing, in press.

28. Wang, W., J. Li, Z. Yu, Y. Ding, W. Xing, and W. Lu, 2018: Satellite retrieval of actual evapotranspiration in the Tibetan Plateau: Components partitioning, multidecadal trends and dominated factors identifying. J. Hydrol., 559, 471 485, https://doi.org/10.1016/j.jhydrol.2018.02.065

29. I1: http://www.fao.org/3/X0490E/x0490e0b.htm#TopOfPage
30. I2: https://www.esri.com/arcgisblog/products/product/imagery/band-combinations-for-landsat-8/